J Mater Sci (2008) 43:1406–1420
DOI 10.1007/s10853-007-2282-6

PET recycled and processed from flakes with different amount of water uptake: characterization by DSC, TG, and FTIR-ATR

Adhemar Ruvolo-Filho · Priscila S. Curti

Received: 25 July 2007 / Accepted: 30 October 2007 / Published online: 12 December 2007
© Springer Science+Business Media, LLC 2007

Abstract Recycled PET from bottles was processed from flakes, which containing different amounts of water uptake. After this process, they are subjected to characterization by differential scanning calorimetry (DSC), thermogravimetry (TG), and Fourier-transform infrared spectroscopy with an attenuated total reflectance accessory (FTIR-ATR). From the DSC and TG results it can be postulate an increase in the proportion of short-molecular-weight distribution in the PET chains, due to the hydrolytic degradation of recycled PET during the thermopressing in presence of water. This hydrolytic degradation probably formed more polar groups on the surface of the processed and recycled PET, like carboxyl groups, as observed by FTIR-ATR.

Introduction

Until the 1980s, poly(ethylene terephthalate) (PET) resin was used mainly in the manufacture of textile fibers, but since this time, occurred the increasing in the processing of PET to manufacture plastic bottles for drinks such as water, juice, soft drinks, etc. These PET bottles have a short life-cycle and they are quickly discarded into the municipal waste system, whose the accumulation occurs. Thus, the recycling of PET post-consumer bottles is vital to diminish the environmental pollution, as the natural degradation of PET takes a very long time. Another advantage of PET recycling is the enhanced value of the reprocessed material, as well the creation of jobs.

Brazil is the country with the greatest percentage of post-consumer PET recycling in the world, surpassing the United States and Europe. In 2005, Brazil used 374 thousand ton of PET resin to produce bottles and recycled 174 thousand ton, corresponding to 47% of recycling, which was the same percentage achieved in 2004, when in Brazil 360 thousand tons of PET resin was consumed to produce bottles and 167 thousand tons were recycled [1, 2]. In this country, the main method used to recycle PET is mechanical recycling. In this method, the PET is submitted to physical transformations during the processing, and the resin obtained is destined for manufactured products with poorer mechanical properties, than the virgin PET resin and consequently have a lower aggregated value. For example, some materials produced from recycled PET are bottles for non-food products, ropes, bristles for brushes and brooms, carpets, TNT (textile non-textile), etc.

La Mantia et al. [3] and later Torres et al. [4] associated the loss in the mechanical properties of recycled PET with the number of processing cycles. The former [3] studied the change in the mechanical properties of PET bottles as a function of the number of extrusions and they verified that their properties worsen with successive PET bottles extrusion. They related this phenomenon to the scission of PET molecule backbones, due to thermo-mechanical degradation. The latter authors [4] also showed that after the injection process, the mechanical properties of post-consumer PET contaminated with PVC were poorer than the mechanical properties of virgin PET. They attributed this result to the humidity and contaminants present in the post-consumer PET, which promoted scissions in the post-consumer PET chains and diminish the intrinsic viscosity of the polymeric material.

A. Ruvolo-Filho (✉) · P. S. Curti
Group of Processing and Properties in Polymer, Department of Chemistry, Center of Exact Sciences and Technology, Federal University of São Carlos, P.O. Box 676, São Carlos, SP 13565-905, Brazil
e-mail: adhemar@power.ufscar.br

Another technique of mechanical recycling of is known as bottle-to-bottle, in which post-consumer bottles are reused in direct contact with food. This technique involves the steps of adequate washing, decontamination, crystallization, and post-condensation in the solid state of PET post-consumer bottles. In the United States and in some countries of Europe, the bottle-to-bottle technique is allowed and some processes are patented, such as the Supercleaning™ and Supercycle [5], etc. However, in Brazil, the Regulation No. 105 of ANVISA (Agência Nacional de Vigilância Sanitária, National public health authority) does not allow recycled plastics to be used in direct contact with food, except those reprocessed during the same transformation [6].

For these reasons, chemical recycling is an interesting option, because by using controlled chemical reactions, PET bottles can be broken down into monomers, which can be used to produce virgin PET resin or in the paint industry. Thus, there is a challenge to develop depolymerization methods that are efficient and cheap. In order to enhance this efficiency, it is necessary to increase the reactivity of the reaction medium. In the literature, there are reports of attempts to attain this goal by using concentrated solutions [7–9], high pressures [10–12], supercritical conditions [13–15] or using a mixture of reactants [16–18]. However, these reaction conditions are harsh and make the chemical recycling of PET costly. An alternative approach to improving the efficiency of PET depolymerization is to try to enhance the initial reactivity of the PET samples that will be used in the depolymerization process, for example, by increasing the number of polar groups in the polymer chains. This can be done by promoting a mild degradation in the PET post-consumer chains.

Villain et al. [19] have studied the thermal and thermooxidative degradation of PET, using thermogravimetric analysis, TG. They detected the volatile products formed during PET degradation, with a Gas Chromatograph connected in line with the TG equipment. The analyses were carried out in isothermal conditions, between 280 °C and 310 °C, because this is the range of temperatures reached inside the mold during the PET injection process. These authors showed that an atmosphere of air intensified the degradation of PET. In this case, the main volatile products were formaldehyde and acetaldehyde. The latter is predominant during the first 2 min of reaction, which is the medium residence time of the PET in the injection mold. These authors also evaluated the influence of humidity in the PET samples during the reaction and found that up to 0.5% humidity, the degradation of PET was not influenced by this parameter. However, values above 0.5% influenced the subsequent PET degradation, which was intensified by this amount of water present in the PET, which acted as an agent of hydrolytic degradation of this polymer.

The formation of acetaldehyde as a product of PET degradation was also observed by Ruvolo-Filho and Carvalho [20], using FTIR spectroscopy. From the FTIR spectrum of a film of PET, previously submitted to heating at 230 °C for 48 h in air, compared with the spectrum of the PET film saturated with acetaldehyde and the spectrum of pure acetaldehyde, they verified that acetaldehyde was formed in the PET film under these severe temperature conditions.

Edge et al. [21] and Dzieciol et al. [22] have also evaluated the products formed during PET degradation. Edge et al. [21] used pellets of virgin PET, which were heated in tubes at 300 °C for 24 h in an air or N_2 atmosphere. After this treatment they estimated the degradation products by luminescence, FTIR, and UV–vis techniques. Their results led them to suggest that in the reaction conditions used, the degradation of PET occurred preferentially by the hydroxylation of the aromatic ring or by quinone formation (the latter is less probable). Dzieciol et al. [22] studied the thermooxidative degradation of post-consumer PET granules obtained from bottle processing, which were free of any kind of contaminant. These reactions were carried in a tubular oven in an airflow of 0.025 m^3 h^{-1}. The time of reaction was 20 min between 200 °C and 700 °C. A gas chromatograph connected to the tubular oven was used to evaluate the composition and concentration of the volatile products of PET degradation. They found that the main volatile products were acetaldehyde, formaldehyde, and carbon monoxide (CO). The concentration of these products rose with the temperature. Thus, these authors concluded that during PET degradation a primary degradation occurs, forming carboxylic and vinyl esters groups. The products of the primary degradation can suffer a secondary degradation that is intensified as the temperature rises, and can form oxides, aldehydes, and aromatic hydrocarbons.

Campanelli et al. [23] studied the hydrolytic depolymerization of the melting virgin PET resin between 250 °C and 280 °C, with an excess of water and without catalytic agents. They used a first-order model in the kinetic study of this reaction, taking the water concentration to be constant during the depolymerization, as it was five times higher than the PET concentration. On the other hand, Kao et al. [10] also studied the hydrolytic depolymerization of melting PET in a stirred controlled reactor, at 235, 250, and 265 °C, under pressure and using water as a hydrolytic agent. They observed that the carboxylic groups formed during the reaction acted as catalysts and decided to use an autocatalytic kinetic model, due to the increase in the number of carboxylic groups during the PET depolymerization. They observed that this model fitted the experimental data well.

Ruvolo-Filho and Soares [24] obtained a patent for a method to depolymerize PET flakes from post-consumer

bottles. In this method the flakes were immersed in excess water for a minimum of 10 days and then processed by thermopressing. They showed that the extent of the reaction was reached just after 10 min at 170 °C, using a nonaqueous ethylene glycol solution of 1.1 mol L^{-1} NaOH. They also showed that the solid product (terephthalic acid, TPA) and the liquid product (ethylene glycol, EG) were produced in high yields and purity. It would be interesting to apply this depolymerization method on the industrial scale, because the TPA and EG could be used as raw materials for virgin PET synthesis or to manufacture new polyester resins used in paint manufacture. In more recent studies, Ruvolo-Filho and Curti [25, 26] found that the apparent depolymerization rate constants obtained from the kinetic study of samples of post-consumer PET processed using flakes previously immersed in water until the saturation, and assuming a heterogeneous reaction medium (temperatures between 150 °C and 185 °C), were higher than the rate constants found in the literature [8, 11, 18, 27–29]. These results indicated that the degradation during processing in the presence of water can enhance the reactivity of the depolymerization reaction more than using drastic reaction conditions in the reaction medium, as described above.

In this context, the aim of this study is to characterize the recycled PET processed from flakes with different amounts of water uptake, using differential scanning calorimetry (DSC), thermogravimetry (TG), and Fourier-transform infrared spectroscopy with an attenuated total reflectance accessory (FTIR-ATR).

Experimental

Materials

Commercial flakes of recycled PET from post-consumer bottles were obtained from Embrapol (Brazil). The flakes of recycled were cleaned with detergent, rinsed in abundant water and dried in an oven. After cleaning, the flakes were stored in a closed room, at 23 °C and air humidity around 70%. Pellets of virgin PET S80 resin were obtained from Mossi & Ghisolfi Group (Brazil). Commercial grade sodium hydroxide (NaOH) and ethylene glycol (EG) were used as received, without further purification.

Initial treatment of the flakes of recycled PET and pellets of virgin PET

Three kinds of initial treatment were carried out on the flakes of recycled PET in order to evaluate whether any hydrolytic degradation takes place during the thermal processing: (i) flakes of recycled PET which were submitted to the crystallization and drying in a controlled oven at 180 °C for 4 h (Sample A). According to Carvalho, de G. M. [30] this thermal treatment is sufficient to enhance the maximum crystallization index of the PET; (ii) flakes of recycled PET which were stored at 70% relative humidity at 23 °C (room temperature) up to the moment of use, and were not dried (Sample B); (iii) flakes of recycled PET which were saturated by immersion in water for a minimum of 10 days at 23 °C, and were not dried before the use (Sample C). In a previous study, Ruvolo-Filho and Soares [24] showed that the immersion of the flakes of recycled PET in water during 10 days is sufficient to reach the maximum water uptake by this material. Also, pellets of the virgin PET S80 resin, previously crystallized and dried in a controlled oven at 180 °C for 4 h, were used for comparison (Sample D).

Table 1 shows these abbreviations just cited above and other that will be cited in this work.

Estimate of the amount of water taken up by the flakes of recycled PET and by the pellets of the virgin PET

The amount of water taken up by the flakes subjected to the three initial treatments mentioned above was estimated by thermogravimetry (TG) using a TG 2050 (TA Instruments). The experimental conditions were: heating rate of 10 °C min^{-1}, N_2 flow rate of 10 mL min^{-1} in the thermobalance and 90 mL min^{-1} in the furnace. The weigh of 19.2 ± 0.2 mg of each material (Samples A, B, C, and D) was placed on a platinum crucible.

Processing of the flakes of recycled PET and of the pellets of virgin PET by thermopressing

Flakes of recycled PET and pellets of virgin PET, pretreated under the three initial conditions as described, were introduced into a metal mold of 6 cm width, 7 cm length, and 0.27 cm thickness, between two Kapton films and two metal plates. The system (metal plate/Kapton film/mold with the polymer/Kapton film/metal plate) was introduced into a Carver hydraulic press, previously heated at 260 °C, and each material was processed identically: the polymer was completely melted at 260 °C after 11 min without pressure; after this melting time, a pressure of 0.5 metric ton was applied and immediately released; finally a pressure of 1 metric ton was applied for 30 s and then released. After this step, the system was quenched at 0 °C to obtain the plates in a vitreous state. The polymer plates prepared by this thermopressing were denominated Samples E, F, G, and H, as cited on Table 1. These samples were stored in a

Table 1 Abbreviations of the samples used in this work

Material	Indication in the text
Flakes of recycled PET which were submitted to the crystallization and drying in a controlled oven at 180 °C for 4 h (PETWD)	Sample A
Flakes of recycled PET which were stored at 70% relative humidity at 23 °C (room temperature) up to the moment of use, and were not dried (PETWH)	Sample B
Flakes of recycled PET which were saturated by immersion in water for a minimum of 10 days at 23 °C, and were not dried (PETWS)	Sample C
Pellets of the virgin PET S80 resin which were crystallized and dried in a controlled oven at 180 °C for 4 h (PETVD)	Sample D
Flakes of recycled PET which were submitted to the crystallization and drying in a controlled oven at 180 °C for 4 h and after were submitted to thermopressing at 260 °C for 11 min (PETWDT)	Sample E
Flakes of recycled PET which were stored at 70% relative humidity at 23 °C (room temperature) up to the moment of use, and were not dried and after were submitted to thermopressing at 260 °C for 11 min (PETWHT)	Sample F
Flakes of recycled PET which were saturated by immersion in water for a minimum of 10 days at 23 °C, and were not dried and after were submitted to thermopressing at 260 °C for 11 min (PETWST)	Sample G
Pellets of the virgin PET S80 resin which were crystallized and dried in a controlled oven at 180 °C for 4 h and after were submitted to thermopressing at 260 °C for 11 min (PETVDT)	Sample H
Flakes of recycled PET which were saturated by immersion in water for a minimum of 10 days at 23 °C, and were not dried and after were submitted to thermopressing at 260 °C for 11 min and later were submitted to an additional thermal treatment at 180 °C for 4 h (PETWSTT)	Sample I
Pellets of the virgin PET S80 resin which were crystallized and dried in a controlled oven at 180 °C for 4 h and after were submitted to thermopressing at 260 °C for 11 min and later were submitted to an additional thermal treatment at 180 °C for 4 h (PETVDTT)	Sample J

freezer until the use. Samples G and H were later submitted to an additional thermal treatment at 180 °C for 4 h and denominated Samples I and J, respectively.

Characterization of processed materials

Differential scanning calorimetry (DSC)

DSC analysis was used to determine the thermal properties (transition temperatures, the enthalpies of these transitions and the crystallinity index) of the Samples E, F, G, H, I, and J and a comparative study was carried out. For these analyses the samples cited were cut into transverse sections and weighing 5.61 ± 0.02 mg. The analyses were performed with a DSC 2010 (TA Instruments), using a hermetic aluminum crucible with a N_2 flow rate of 75 mL min^{-1} and a heating rate of 10 °C min^{-1}.

Study of thermal and thermooxidative decomposition by thermogravimetric analysis (TG)

The thermal and thermooxidative decomposition of the Samples F, G, and H was investigated by a non-isothermal kinetic method, in order to test the influence of the atmosphere on the decomposition profile of these samples.

These samples were cut into transverse sections weighing 19.5 ± 2 mg, which were previously dried in a controlled vacuum oven at 50 °C for 15 h to eliminate humidity (that could be interfere with the shape of the TG thermal curves). The equipment used was a TG 2050 (TA Instruments), with a platinum crucible. Nitrogen flowing at 15 mL min^{-1} was used in the thermobalance, while both N_2 and O_2 were used in the furnace, flowing at 95 mL min^{-1}. The experiments were carried out at heating rates of 10, 15, 20, 30, and 40 °C min^{-1}.

The non-isothermal kinetic study was carried out, as described, in ASTM E1641-99 standard method [31]. From the TG thermal curves of loss of mass versus temperature, at the various heating rates cited, isopleths were traced for conversions, α, between 5% and 70% over the correspondent absolute temperature of decomposition. These values were used to find the relation between α and the reciprocal of the absolute temperature, for each heating rate cited. The ASTM E1641-99 [31] uses the Ozawa method to determine the activation energy, E_a, of the decomposition process, according the equation:

$$\log \beta = -0.457\left(E_a/RT\right) \quad \text{or} \quad \ln \beta = -1.0511\left(E_a/RT\right) \tag{1}$$

where $\ln\beta$ is the natural logarithm obtained from each heating rate, β, used in this work; E_a is the activation energy of the thermal or thermooxidative decomposition;

R is the gas constant; and T is the absolute temperature at which a given conversion, α, occurs.

The Ozawa method is valid if the α versus $1/T$ plot, for different heating rates, can be superposed. This was tested for each material used and the superposition results were good, indicating that this method is valid for these samples. Thus, the linear regression of $\ln\beta$ versus $1/T$ (K) data was carried out by Eq. 1. Applying the iterative method described in ASTM E1641-99 [31], the E_a values were determined and refined. The Arrhenius pre-exponential factor, A, is calculated from Eq. 2, according to ASTM E1641-99 [31].

$$A = -(\beta'/E)R\ln(1-\alpha)10^{a} \quad (2)$$

The thermal and thermooxidative decomposition results of the various samples cited above were compared, to reveal possible correlations of the variation in E_a and A values with the molecular-weight distribution and differences in the interactions of samples with the gas used in the furnace during the analysis.

Fourier transform infrared spectroscopy with the attenuated total reflectance accessory (FTIR-ATR) analysis

FTIR-ATR analysis was used to make a comparative evaluation of the possible variation in the relative percentage of the carbonyl groups on the surfaces of the Samples E, F, and G. The FTIR Nicolet Protégé™ 460 Spectrometer was used. The samples used in this study were 70 μm and 270 μm thick films of Samples E, F, G, and H. The spectra were obtained using 256 scans and 4 cm^{-1} resolution. An ATR accessory (horizontal mode), consisting of the ZnSe crystal, with the beam at a constant angle of incidence of 45°, was used to obtain the spectra. Before each spectrum, the analysis chamber was purged with compressed air for 30 min. N_2 was also used as purge gas for comparison with the compressed air results.

The absorption intensity of the band at 1,715 cm^{-1}, related to the absorption of the carbonyl groups in α-β-unsaturated compounds, was estimated for each sample.

Sammon et al. [32] have studied the degradation of virgin PET films immersed in water at 90 °C for between 4 and 8 days. These authors used the Reflection Absorption Infrared Spectroscopy (FTIR-RAIRS) technique and from the spectra obtained, found no evidence of degradation reactions in the aromatic rings in the PET films, under the reaction conditions used. Thus, the authors assumed that the absorption band at 1,410 cm^{-1}, related to the CH groups of the aromatic ring, could be used as an internal reference absorption band, in order to normalize the intensity of the band related to the OH groups, between 3,200 and 3,500 cm^{-1}, so as to eliminate possible thickness effects. Therefore, the rise in the relative normalized absorption intensity, in the OH group range, was related to the degradation process that occurred in the PET films.

For these reasons, the absorption intensity of the band at 1,410 cm^{-1} has also been used as an internal reference, in order to eliminate a possible thickness effect, assuming no reaction occurs in the aromatic rings in the PET chains, during the processing of the flakes of recycled PET and the pellets of virgin PET by thermopressing.

A relative comparison of the normalized absorption intensity band at 1,715 cm^{-1} obtained from the Samples E, F, and G was made with reference to normalized absorption intensity band at 1,715 cm^{-1} obtained for the Samples H.

Results and discussion

Water taken up by the flakes of recycled PET and by the pellets of virgin PET

The amount of water taken up by the flakes of the recycled PET samples (Samples A, B, and C) was estimated by TG analysis. Water uptake was deduced from the thermal TG curves of percent mass loss, between room temperature and 210 °C (given that in this interval of temperature, any water taken up by the flakes could be totally eliminated during the heating of the sample at 10 °C min^{-1}). The results of this analysis are presented in Table 2, and it can be seen that the process of crystallization and drying of the flakes of the recycled PET and pellets of virgin PET at 180 °C for 4 h is sufficient to eliminate all the water taken up by the polymer. On the other hand, when the flakes of the recycled PET are stored at room temperature and 70% relative humidity, the amount of water taken up is around 0.2%, and when they are immersed in excess water for a minimum of 10 days, which is sufficient for the uptake of water to reach its maximum [24], the amount of water taken up is around 0.8%.

In order to evaluate the influence of the amount of water taken up initially by the flakes of recycled PET on the properties of the processed samples (Samples E, F, and G)

Table 2 Estimated amount of water taken up by the pellets of virgin PET (Sample A) and the flakes of recycled PET subjected to the three distinct initial treatments (Samples A, B, and C)

Sample	Water uptake (%)
D	0.0
B	0.2 ± 0.1
A	0.0
C	0.8 ± 0.1

in comparison with the Samples H, DSC, TG, and FTIR-ATR analyses were carried out on these samples and the results are shown next.

Differential scanning calorimetry (DSC) analysis

In Fig. 1 are presented the DSC thermal curves of the Sample H (Fig. 1(a)), Sample E (Fig. 1(b)), Sample F (Fig. 1(c)), and Sample G (Fig. 1(d)), in the vitreous state, and after to submit the Samples G and H to a thermal treatment 180 °C for 4 h, Samples I and J, (Fig. 1(e, f)).

The crystallization enthalpy (ΔH_c) and the melting enthalpy (ΔH_m) were determined by tracing just one base line from the beginning of the exothermic process to the end of the endothermic process. This approach was adopted in light of the Khanna and Kuhn [33] observations, which were confirmed by Carvalho, de G.M. [30] for PET, that once the temperature of amorphous and crystallizable polymer attains the glass transition temperature, T_g, and rises toward the melting temperature, T_m, events of crystallization/recrystallization occur and the crystallites present in the polymer become more perfect until the total melting of the polymer at T_m. Therefore, the base line needs to include the whole A–B interval indicated in the DSC thermal curves in Fig. 1, in order to take the equilibrium of the crystallization/recrystallization events between the T_g and T_m into account.

The values of these thermal properties, estimated for each of the processed are presented in Table 3. It is seen that the T_g of the material falls as the amount of water taken up by the flakes rises. Also, the Samples E, F, and G have lower T_c values than that the Sample H, and fall appreciably with increasing water uptake before thermo-pressing. On the other hand, the ΔH_c value increases with the amount of water taken up. As can be observed in Table 3, the T_c for Sample G is 23 °C lower than the value

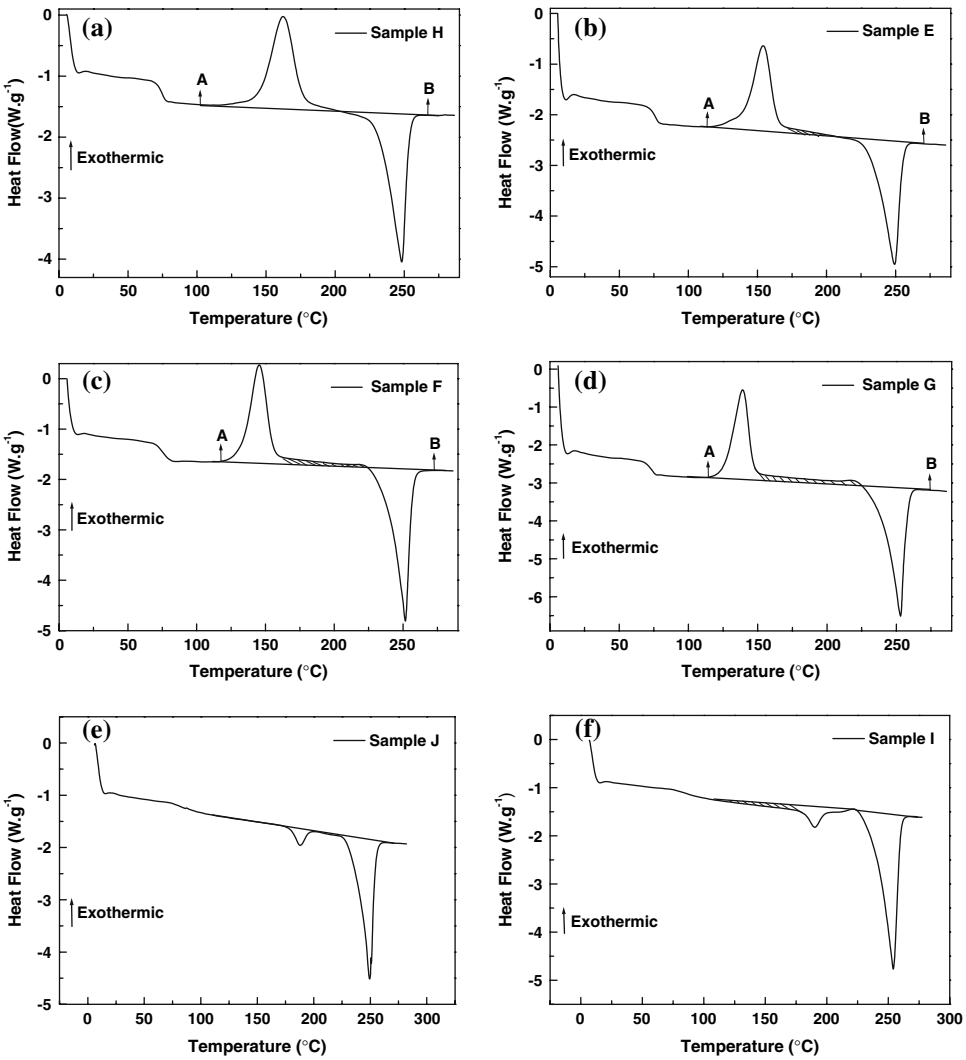

Fig. 1 DSC thermal curves of (**a**) Sample H, (**b**) Sample E, (**c**) Sample F, (**d**) Sample G, (**e**) Sample I, and (**f**) Sample J

Table 3 Estimated glass transition temperature, T_g; crystallization enthalpy, ΔH_c; maximum crystallization temperature, T_c, and melting enthalpy, ΔH_m, for endotherm I and endotherm II and the crystallinity index for the Samples E, F, G, H, I, and J

Sample	Water uptake (before thermopressing) (%)[a]	T_g^b (°C)	ΔH_c^c (J g^{-1})	T_c^c (°C)	ΔH_m^c (J g^{-1}) Endotherm I	T_m^c (°C) Endotherm I	ΔH_m^c (J g^{-1}) Endotherm II	T_m^c (°C) Endotherm II	χ_c (%)
H	0.0	77.6	34.6	162.0	–	–	36.0	248.3	1.1
E	0.0	76.5	33.1	154.2	–	–	36.9	249.3	2.9
F	0.2 ± 0.1	75.4	36.8	145.5	–	–	40.0	251.7	2.5
G	0.8 ± 0.1	75.4	43.1	139.2	–	–	46.3	253.1	2.5
J	0.0	–	–	–	3.5	187.8	34.8	249.5	29.5
I	0.8 ± 0.1	–	–	–	11.9	190.1	47.4	254.1	45.8

[a] Estimated from the TG thermal curves

[b] Values estimated from the second DSC thermal curve scan (after the first scan to the melting point and quenching in ice)

[c] Values estimated from the first DSC thermal curve scan

for the Sample H, while the ΔH_c for former is 8.5 J g^{-1} higher than the latter. These results indicate the occurrence of a process of hydrolytic degradation in the polymeric material during thermopressing that depends on the amount of water taken up by the flakes before the processing. Thus, the tendency to increase the proportion in the chains of short molecular-weight distribution during thermal processing of PET is stronger when the flakes have taken up more water. Observing the base line traced between T_g and T_m on the DSC thermal curves (interval A–B in graphs of Fig. 1), one remaining exothermic heat flow is seen in the Samples E, F, and G (hatched area in Fig. 1(b–d), which is practically negligible in the Sample H (Fig. 1(a)), in which the polymer melting (endothermic peak) is initiated as soon as the crystallization (exothermic peak) is finished. In the DSC thermal curves presented, this phenomenon was more visible in Sample G, that is, in flakes that had previously been immersed in water until saturation and then subjected to thermopressing. This result is one more indication that during thermopressing the hydrolytic degradation was more intense in Samples G and the proportion of short chains in these samples was higher than in Samples H. The latter probably have a molecular-weight distribution rich in long chains, because probably they did not suffer hydrolytic degradation during the thermopressing.

Carvalho, de G.M. [30] has used density, sorption, WAXD, FTIR, and DSC measurements to study the behavior of semicrystalline PET at different temperatures and for various thermal treatment times. These authors observed that the amorphous regions of PET consists of two phases: a mobile amorphous phase (MAP), in which the PET chains are entirely disorganized, and a rigid amorphous phase (RAP), where the PET chains exhibit 2D organization over short distances. Semicrystalline PET also has a crystalline phase, with 3D organization over long distances, and the X phase, constituted by imperfectly crystalline trans isomers (this region shows more organization than the RAP, but the crystallites have not yet been incorporated into the lamella of the 3D crystals). During the thermal treatment of semicrystalline PET, both MAP and RAP phases can crystallize to form the X phase and/or enlarge the 3D crystalline phase. Carvalho, de G.M. [30] found that when PET is submitted to thermal treatment beyond 180 °C, the energy supplied to the PET is sufficient for the RAP to become more mobile and form more ordered structures. Parallel to this, the formation and improvement of crystals from the MAP occurs and the X phase is formed. Under these thermal treatment conditions, the mesomorphic phase, an intermediary 2D crystalline state (imperfect), is constituted only of the X phase and the amorphous phase has no influence on the DSC analysis, since this phase is not present after the thermal treatment at 180 °C. This ensures that the value of the melting enthalpy of the mesomorphic phase (endotherm I) is due only to the melting of the X phase.

In view of these hypotheses proposed by Carvalho, de G.M. [30], in the present study, the thermal behavior of the Samples J and I was evaluated by analyzing their DSC thermal curves, which are shown in Fig. 1(e, f), respectively. The values of the T_m and the ΔH_m related to the endotherms I and II are presented in Table 3. In these curves it is observed that the temperature range of the endotherm I for the Sample I is more extended than that Sample J. Thus, during the DSC scan the short-chain crystals present in Sample I probably melt at lower temperatures (hatched area in Fig. 1(f)), while the mesomorphic phase melts at the endotherm I peak, at 190.1 °C. Analyzing the DSC for the Sample J, only the melting of the mesomorphic phase is seen, producing endotherm I at 187.8 °C, probably because the molecular-weight distribution of long chains is more uniform, without the presence of short chains. Therefore, it can be suggested that the Samples C (before the thermopressing and thermal treatment) suffer greater hydrolytic degradation during thermopressing, compared with the Sample D (before the thermopressing and thermal treatment), because the amount

of water taken up by the former is much more than by the latter.

The crystallinity index, χ_c, was also estimate from the DSC analyses using the following relation:

$$\chi_c = \frac{\Delta H_m - \Delta H_c}{\Delta H_{m,100\%}} \times 100 \quad (3)$$

where ΔH_m is the melting enthalpy of the whole material, obtained from the DSC analysis, ΔH_c is the crystallization enthalpy of the whole material, obtained from the DSC analysis and $\Delta H_{m,100\%}$ is the melting enthalpy value, obtained from the DSC analysis, related to the material considered 100% crystalline. Carvalho, de G.M. [30] obtained the value of $\Delta H_{m,100\%}$ 130 J g^{-1} for pellets of virgin PET, which is the same material used here; thus, this value was used to estimate the χ_c, in this study.

The results are presented in Table 3. These confirm the small values of χ_c, expected for the amorphous samples. After the thermal treatment of the Samples G and H at 180 °C for 4 h (Samples I and J), their χ_c values increased, especially in the Sample I. Therefore, it can be inferred that the χ_c values estimated from DSC analysis indicate greater mobility in the chains of the Sample G, during the thermal treatment, due to the bigger proportion of short molecular-weight distribution of chains than in the Sample H, favoring the ordering of these polymeric segments. Other explanation for this behavior is the possibility of formation of a higher fraction of polar groups in the Samples G than in Samples H. This higher fraction of polar groups in the Sample G could rises the tendency of this Sample to crystallizes.

Analysis of thermal and thermooxidative decomposition

The kinetic TG study of the thermal and thermooxidative decomposition of the Samples F, G, and H was carried out in conformity with ASTM E1641-99 [31], adopting the non-isothermal method. According to standard, relatively high heating rates could influence the determination of the mass-loss temperatures for the initial conversion values, due to the changing mass loss of volatile fractions during the analyses. Thus, in order to avoid this behavior in the TG curves, some TG analyses were performed on pellets of virgin PETV, both without processing (Sample D) and then following the thermopressing (Sample H) and also on Sample G, at heating rates of 5 °C min^{-1} and at 10 °C min^{-1}. The TG thermal curves are presented in Fig. 2. In all TG thermal curves there is an initial apparent mass increase followed by an apparent mass loss. According to manufacturer's data [34] the TG thermobalance has a nominal precision of 0.1% of the weight. Thus, only mass changes higher than 0.1% are significant. Estimating the loss of mass referring to the first interval of loss of mass in the TG thermal curves, it was found that the percentage mass loss was 0.04% for the pellets of virgin PET (at 5 °C min^{-1}), 0.07% for the pellets of virgin PET (at 10 °C min^{-1}), 0.03% for the Sample G (at 10 °C min^{-1}), and 0.02% for the Sample H (at 10 °C min^{-1}). These values of loss of mass are not physically significant, because they are below of the detection limit of the TG thermobalance. Therefore, up to the beginning of the degradation, the changes in the mass are probably due to the convective gas flow in the furnace and it is clear that there is no influence of volatiles on the TG analysis. In view of this result, the TG thermal curves were produced at heating rates of 10, 15, 20, 30, and 40 °C min^{-1}, using N_2 and O_2 as distinct flow gases. Some TG analyses were done in duplicate. ASTM E1641-99 [31] assumes that the decomposition conforms to a first-order kinetic model. According to Hatakeyama [35] the thermal or thermooxidative decomposition of polymers can be analyzed by a non-isothermal kinetic method, and kinetic parameters such as the activation energy, E_a, and the Arrhenius exponential pre-factor, A, are then estimated from the following:

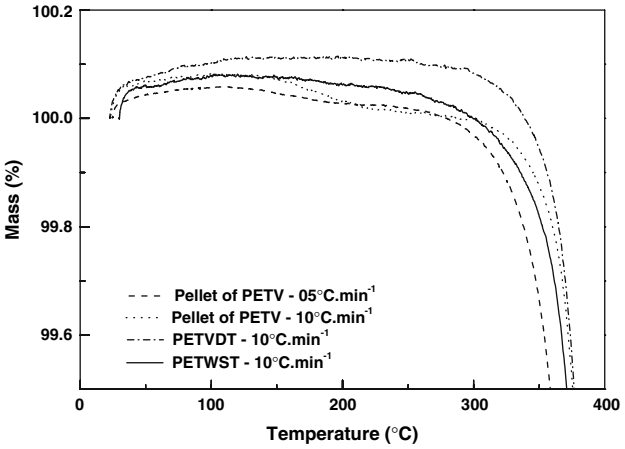

Fig. 2 TG thermal curves of the Samples D, G, and H, using two different heating rates. Before each analysis the samples were dried in a vacuum oven at 50 °C for 15 h

$$\frac{d\alpha}{f(\alpha)} = g(\alpha) = -\frac{A}{\beta}\exp\left(-E_a/RT\right)dT. \quad (4)$$

Equation 4 can be solved by integration:

$$\int_{\alpha_o}^{\alpha}\frac{d\alpha}{f(\alpha)} = g(\alpha) = -\frac{A}{\beta}\int_{T_o}^{T}\exp\left(-E_a/RT\right)dT \quad (5)$$

Doyle suggested that when E/RT value is higher than 20, the following approximation can be made:

$$\log p\left(E_a/RT\right) \approx -2,315 - 0,457\left(E_a/RT\right) \quad (6)$$

The thermal degradation mechanism of PET occurs by random breaks at the ester linkages, to leave terminal carboxyl and vinyl ester groups. The reaction products of primary degradation can suffer secondary degradation, forming carbon monoxide, aldehydes, hydrocarbons, acids, and esters [21, 22]. The reactions of thermooxidative degradation are also complex and still need to be explained. However, it is known that PET stability depends on the kind of catalyst used in the transesterification process and also the amount of diethylene glycol linkages previously broken, which make the polymer more reactive and increase the rate of the reaction [22]. Arii et al. [36] showed the thermal degradation mechanism of PET as corresponding to the random scission of chains, using controlled-rate TG analysis.

Based on these observations, the Doyle method can be simplified by using the Ozawa approximation, assuming random scission of PET chains and that plots of the conversion, α, against reciprocal absolute temperature, should be parallel lines for the various heating rates. If this behavior occurs, a master curve can be obtained from the superposition of the α versus $1/T$ lines. Thus the Ozawa approximation can be applied and Eq. 6 becomes:

$$\log \beta = -0.457\left(E_a/RT\right) \quad \text{or} \quad \ln \beta = -1.0511\left(E_a/RT\right). \tag{7}$$

This equation is identical to Eq. 1, seen in the experimental section. The ASTM E1641-99 method makes use of Eq. 7 and an iterative method to determine the E_a value, which has explained in detail in the experimental section. The value of A is determined from Eq. 2.

In Fig. 3(a) are presented the TG thermal curves for the PETVDT samples, using O_2 as flow gas, at various heating rates. From the isopleths traced, (dotted lines) between 5% and 70% conversion, across these TG thermal curves, the α versus $1/T$ plots were obtained (not shown here). By superimposing the α versus $1/T$ curves, as shown in Fig. 3(b), the validity of the Doyle integration method and the Ozawa approximation, used in this study, were verified. The initial scatter in the α versus $1/T$ data. However, above 40% conversion, the scatter increases (Fig. 3(b)), indicating that the estimates of E_a and A are reliable only in the early stages of the thermooxidative decomposition. According to the ASTM E1641-99 method [31], the value of E_a can be determined up to 20% conversion. Beyond this point, the reaction can become unstable and the determination of E_a less reliable. Using the α versus $1/T$ data at each heating rate, the relation between $\ln\beta$ and $1/T$ was found, as presented in Fig. 3(c). From this relation (up to 17.5% conversion) E_a, and A were calculated for the Sample H using Eqs. 1 and 2 and the iterative method proposed in ASTM E1641-99 [31]. These values are presented in Table 4. According to the literature [22], the thermooxidative decomposition of PET is complex and the steps are not yet well explained.

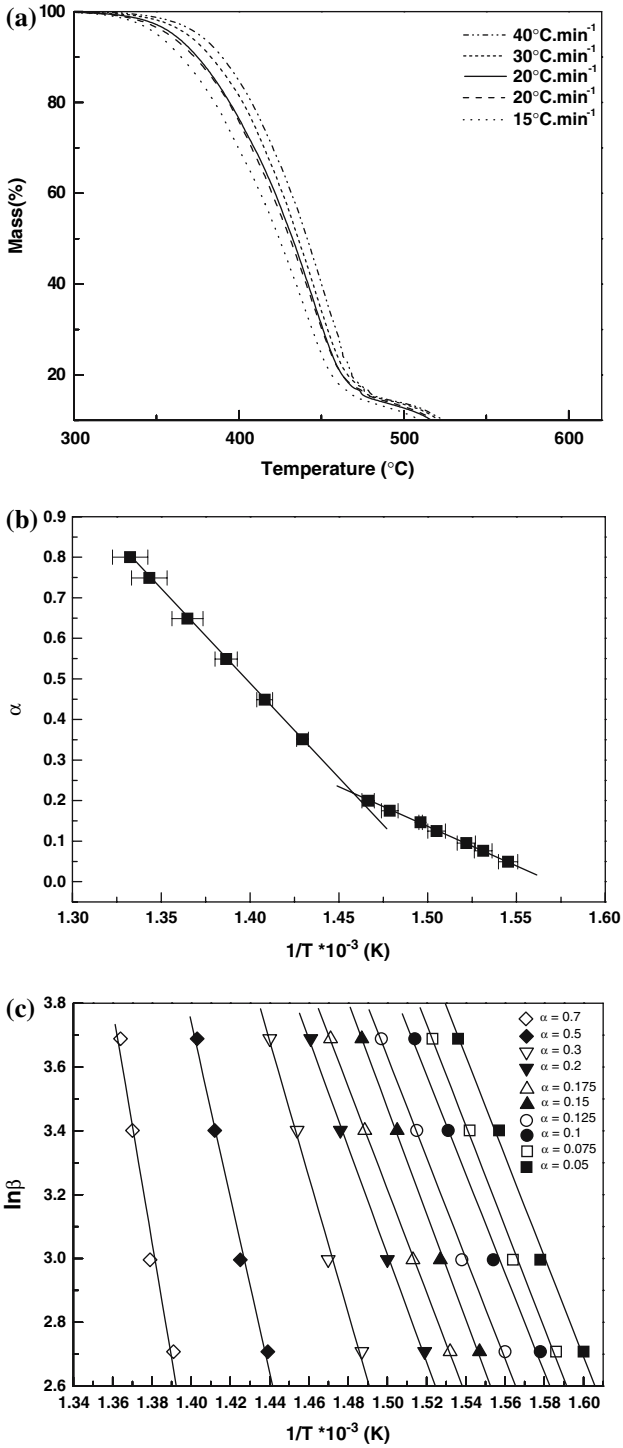

Fig. 3 (**a**) TG thermal curves of Samples H, at heating rates of 15, 20, 30, and 40 °C min^{-1}, in O_2 atmosphere; (**b**) superimposed α versus $1/T$ (K) data by analyzing the TG thermal curves presented in (**a**), and (**c**) $\ln\beta$ versus $1/T$ (K) plots between 5% and 70% conversion

TG thermal curves of Samples G also obtained using O_2 as flow gas (data not shown here). By the same mathematical

Table 4 Estimated mean kinetic values of the E_a and A parameters, obtained from the non-isothermal study of the thermal and thermooxidative decomposition of the Samples F, G, and H, using the method in ASTM E1641-99 [31]

Sample	Gas flowing in the furnace	Limits of interval of conversion (%) used to determine E_a and A values	E_a (kJ mol^{-1})	A (min^{-1})
H	O_2	5–17.5	127.9 ± 2.8	23.5 ± 0.9
G	O_2	5–12.5	176.9 ± 2.3	31.3 ± 0.3
F	O_2	5–12.5	131.8 ± 5.1	23.5 ± 1.1
H	N_2	5–20	281.1 ± 1.0	47.7 ± 0.5
G	N_2	5–15	247.4 ± 4.8	42.65 ± 1.2

treatment, the α versus $1/T$ curves were superimposed this sample at different heating rates, and the data was more scattered from 30% conversion. In Fig. 4, $\ln\beta$ versus $1/T$ plots for Samples G are shown. There is good correlation between these parameters in the initial stages of the thermooxidative decomposition. The mean values of the kinetic parameters, determined in the interval from 5% to 12.5% conversion, are presented in Table 4 and, as can be observed, the errors estimated for the E_a and A values of the Sample G are within acceptable limits.

Comparing the kinetic parameters for the thermooxidative decomposition of Samples G and H (Table 4), an increase of 49 kJ mol^{-1} in the E_a value of the former sample is seen. This result indicates that during the processing of the Sample C to obtain the Sample G, hydrolytic degradation occurs and forms polar groups, such as carboxyl groups, probably mainly on the surface. Thus, hydrogen-bond interactions may occur among the carboxyl groups formed in the PET chains, at the surface of the sample, and the O_2 atmosphere present in the furnace, as indicated schematically in Fig. 5(a). These hydrogen-bond interactions could increase the energy needed to break these interactions in Samples G and start the decomposition process, compared to the Samples H. Other hypothesis to explain the higher value of the E_a determined to the Sample G, compared to the Sample H, in the thermo-oxidative study, is a possibility to the formation of the hydrogen-bond interactions between own carboxyl groups formed on the surface of the Sample G during the thermopressing, as indicated in the Fig. 5(b).

Due to this behavior, the E_a value of Sample G is higher than that of Sample H. However, once the decomposition is initiated, its proceeds rapidly, because the fraction short chains is higher in the Sample G sample than in the Sample H, and thus the former is more unstable.

The same experimental approach and mathematical treatment were applied to the Samples F, when subjected to thermooxidative decomposition. In Fig. 6 are presented the $\ln\beta$ versus $1/T$ curves obtained from the TG thermal curves for Samples F, at different heating rates, with O_2 as flow gas. The properties of this material were found to be intermediate between those of the Sample G and H. As shown in Table 4, the mean values of E_a and A of the Samples G are close the values for the Samples H. This result indicates that the immersion of the flakes of recycled PET in water until saturation (Sample C) is essential to enhance the formation of the carboxyl groups on the surface during thermopressing (Sample G), and consequently increase the interaction between the carboxyl groups on the polymer surface and the reactive atmosphere in the furnace.

In addition, TG thermal curves were obtained with N_2 as flow gas, in order to study the thermal decomposition of Samples G and H in an inert atmosphere and find out

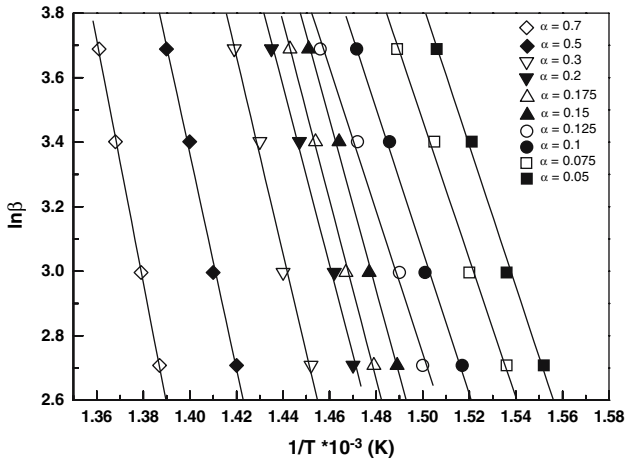

Fig. 4 $\ln\beta$ versus $1/T$ (K) plots between 5% and 70% conversion, derived obtained from the TG thermal curves of the Samples G, obtained in an O_2 atmosphere at heating rates of 15, 20, 30, and 40 °C min^{-1}

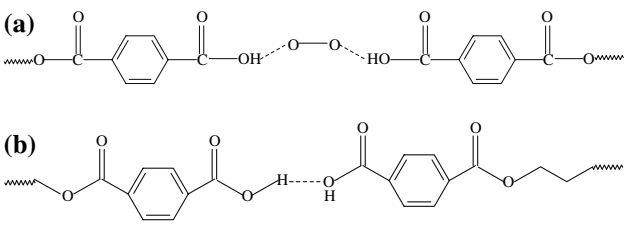

Fig. 5 Illustrative scheme of the possible stabilization of the free carboxyl groups present on the surface of the Sample G through the formation of hydrogen-bonds interactions (**a**) with the O_2 atmosphere in the TG furnace and (**b**) with own free carboxyl groups presents on the surface of the Sample G

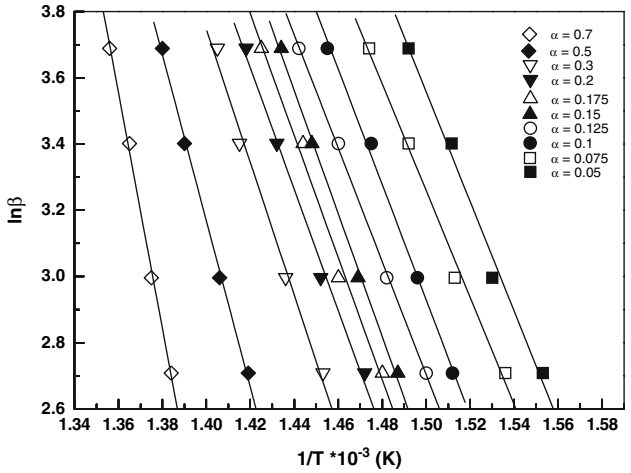

Fig. 6 lnβ versus 1/T (K) plots between 5% and 70% conversion, derived from the TG thermal curves for the Samples F, obtained in an O_2 atmosphere, at heating rates of 15, 20, 30, and 40 °C min^{-1}

whether the formation of polar groups on the surface of the Samples G influences the E_a values under these conditions.

As commented earlier, the thermal degradation of PET is initiated by the random scission of PET chains in the ester linkage, and primary and secondary reactions can occur [22]. The reactions of the primary degradation are shown in the scheme in Fig. 7. N_2 gas is inert and does interact with the sample structure during the TG analysis. Thus, the sample shows greater stability as the temperature in the furnace rises during the heating. This thermal stability increases with the molecular weight of the material.

In Fig. 8 are presented the TG thermal curves of Samples H in N_2 atmosphere (Fig. 8(a)), the superposed α versus 1/T curves for various heating rates (Fig. 8(b)) and the lnβ versus 1/T plots, from 5% to 70% conversion (Fig. 8(c)). The curves presented in Fig. 8(b) show the absence of dispersion in the α versus 1/T data in N_2 atmosphere. The mean values of E_a, determined from the

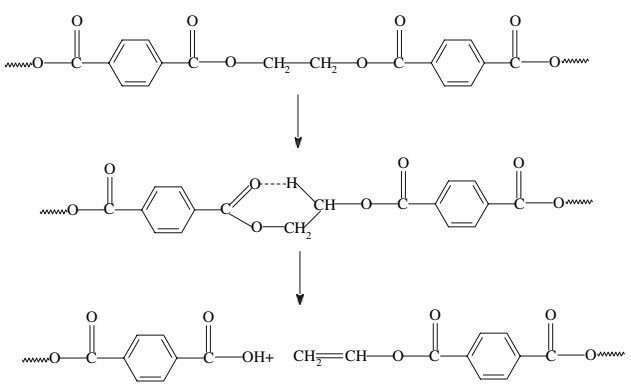

Fig. 7 Illustrative scheme of the reactions leading to the primary degradation of PET chains, in N_2 atmosphere [22]

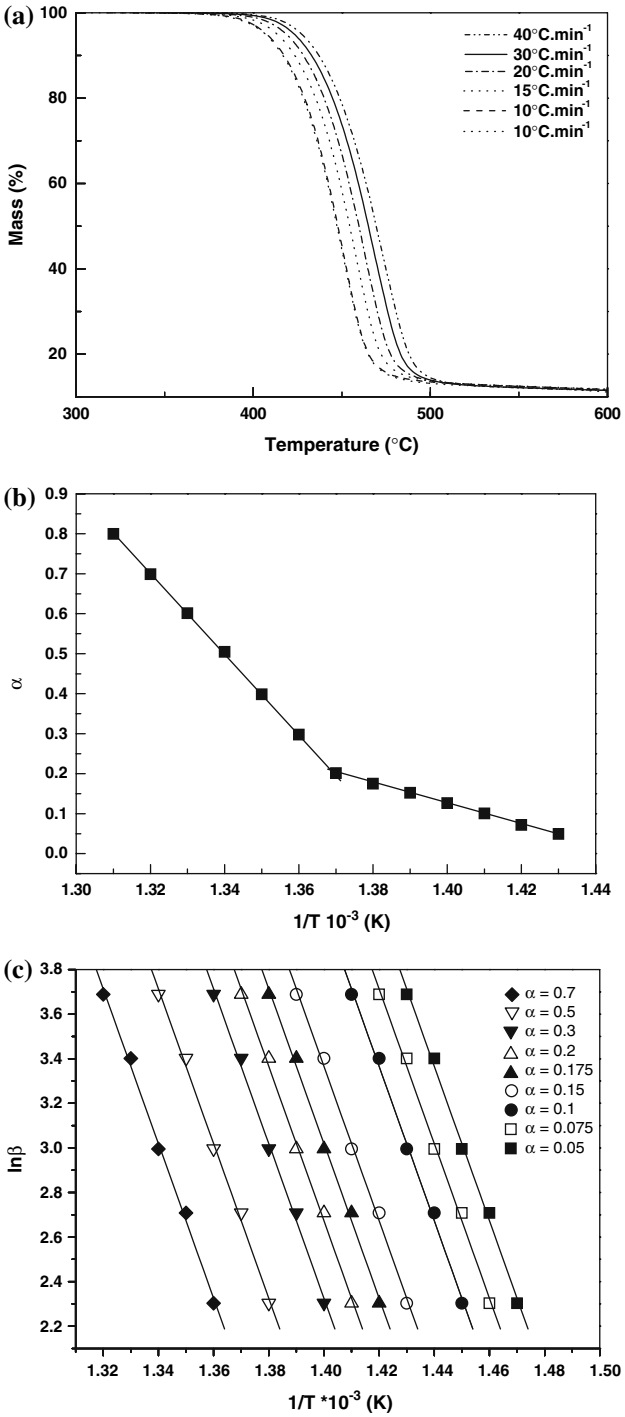

Fig. 8 (**a**) TG thermal curves of Samples H in N_2 atmosphere and at heating rates of 10, 15, 20, 30, and 40 °C min^{-1}; (**b**) superimposed α versus 1/T (K) data, derived from the TG thermal curves presented in (**a**), and (**c**) lnβ versus 1/T (K) plots between 5% and 70% conversion

slope and of A, obtained from the intercept of the lines in Fig. 8(c), are presented in Table 4.

The same experimental approach was also used for the Samples G, in order to make a comparative analysis.

On superimposing the α versus $1/T$ data obtained from the TG thermal curves of the Samples G at different heating rates (results not shown here), a little dispersion was observed in the α versus $1/T$ values. This result probably indicates that the thermal decomposition of this Sample is just a little more unstable than that of Samples H, in the N_2 atmosphere. The $\ln\beta$ versus $1/T$ data for the Sample G are presented in Fig. 9 and the E_a and A values in Table 4. As can be seen in this Table, in a nitrogen atmosphere, the E_a value of the Sample H is 34 kJ mol^{-1} higher than the E_a value of the Sample G. This result, which contrasts with the relative difference between the E_a values of the same materials for thermooxidative degradation, corroborates the initial supposition that polar groups are formed on the surface of the Sample G, by hydrolytic degradation during thermopressing and the proportion of short chains is increased in the chains of the Sample G, compared in the chains of the Sample H. The high proportion of short chains of the Sample G makes its thermal decomposition more unstable than the Sample H, in an inert atmosphere, because the thermal stability is directly related to the molecular-weight distribution in the polymeric material.

In the literature there are several studies of the thermal decomposition of post-consumer PET [37, 38]. Saha et al. [37] have investigated the non-isothermal kinetics of pyrolysis of post-consumer PET from bottles of Coca-Cola and Pepsi. TG analyses were carried out at three different heating rates, with N_2 gas flowing in the furnace. The authors derived the kinetic parameters by two distinct methods: first the ASTM E698 method, which implies that the degradation reaction occurs by a first-order mechanism, considering the calculus of the temperature to be that

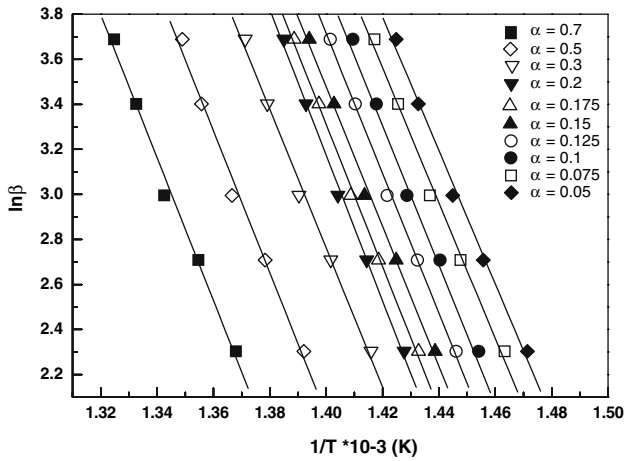

Fig. 9 $\ln\beta$ versus $1/T$ (K) plots between 5% and 70% conversion, derived from the TG thermal curves for the Samples G, obtained in N_2 atmosphere and at heating rates of 10, 15, 20, 30, and 40 °C min^{-1}

corresponding to the absolute temperature at the maximum $d\alpha/dT$ value; in the second method. They considered models of order n, to determine the kinetic parameters and the order of the reaction. The authors observed only one peak in the TG thermal curves, indicating that the degradation process occurs in just one step. In that work, the E_a values, determined from the order n model, were 322.3 kJ mol^{-1} for the post-consumer PET bottles from Coca-Cola and 338.98 kJ mol^{-1} for those from Pepsi. The E_a values obtained by the ASTM E698 method were 162.15 kJ mol^{-1} and 210.64 kJ mol^{-1}, respectively. Thus, the E_a values determined by ASTM E698 were lower than those obtained with the models of order n. The models of n use a large interval of temperature, which covers the temperatures of the initial stages of degradation, while ASTM E698 considers only the temperature corresponding to the maximum in $d\alpha/dT$, that is, in the final stages of the degradation reaction.

In another and more recent work, Saha et al. [38] compared the isoconversion method (Vyazovkin free model) with the non-isothermal study of post-consumer PET bottle. For this method they used various approximation integrals (Coats & Redfern, Agrawal & Sivasubramanian). The TG thermal curves were obtained at four different heating rates, using N_2 atmosphere in the furnace. They determined the E_a and A values by the non-isothermal methods and from the optimum dependence between E_a and α, they observed a good correlation in the integrals of approximation. The results indicate that E_a is a slightly increasing function of conversion, in the case of the non-isothermal decomposition. From the Agrawal & Sivasubramanian approximations used, the E_a values obtained were around 180–210 kJ mol^{-1}.

Probably, the difference in the E_a values obtained for Saha et al. [37, 38] and those determined in this present study, in N_2 atmosphere, are due to the different methods of analysis applied in which work. Also, the differences in the sample preparation methodology used by Saha et al. [37, 38] and in this work should be considered, as they influence the E_a values. Saha et al. [37, 38] cut the PET from the bottles in pieces, without subjecting submitting them to any kind of pretreatment. These pieces of post-consumer PET, weighing 7–10 mg, were introduced directly into the furnace of the TG (Metler TOLEDO) equipment. As already described in this work, the flakes of recycled PET and the pellets of virgin PET were subjected to thermopressing and then cut into samples and subjected to thermal and thermooxidative degradation. This additional step of thermopressing can modify the structural characteristics of the polymer, which can be reflected in the E_a values. However, since the same kinetic model is used to determine the E_a and A parameters for the different materials used, a comparative analysis can be made and the

differences found among them can be considered significant and relevant.

Fourier-transform infrared attenuated total reflectance spectroscopy (FTIR-ATR)

From the results obtained by DSC and TG analyses, presented above, and from the intrinsic viscosity and melt flow index (MFI) measurements, presented in an earlier work [25], it was observed that the thermal processing of the flakes of recycled PET increases the proportion of short chains, specially in the Sample C. According to published reports [19] water promotes degradation of PET at high temperatures. This degradation increases the amount of polar groups, such as carbonyl groups, due to the formation of the carboxyl [10, 23, 32] and aldehyde groups [19, 20] during the processing.

With this in mind, FTIR-ATR was used in order to try estimate comparatively the change in the relative percentages of carbonyl groups on the surfaces of the Samples E, F, G, and H.

The spectral region of 1,715 cm^{-1}, related to the absorption band of carbonyl groups in α-β-unsaturated compounds, was utilized in this study. The intensity of this band can be related to the number of carbonyl groups in the PET macromolecule. Acetaldehyde and formaldehyde, formed as volatile products of PET degradation, do not exhibit the kind of carbonyl group found in α-β-unsaturated compounds, so the analysis of the spectral region of 1,715 cm^{-1} ignores the absorption of the carbonyl groups in acetaldehyde and formaldehyde. On the other hand, this spectral region does reveal ester groups in the main PET chain and the carboxyl groups derived from the hydrolytic degradation of PET during thermopressing. Therefore, any rise in the relative intensity of absorption of the band at 1,715 cm^{-1} is related to the increase in carboxyl groups, due to the hydrolytic degradation of PET.

In Fig. 10 are presented the FTIR-ATR absorption bands around 1,715 cm^{-1}, for Samples E, F, G, and H (films 70 μm thick). In these analyses, compressed air was used as flow gas, in order to eliminate the interference of the carbon dioxide gas in the absorption intensities. Examining Fig. 10, it can be seen that the absorption intensity peak for Sample G is notably higher than the others.

The melting time used in this study during the thermopressing is short, compared with the melting time used by Edge et al. [21], who observed the hydroxylation of the aromatic ring of PET, under several conditions used for PET processing. Villain et al. [19] and Dizieciol et al. [22] also used a short melting time to study the products of PET degradation, but neither authors commented on the

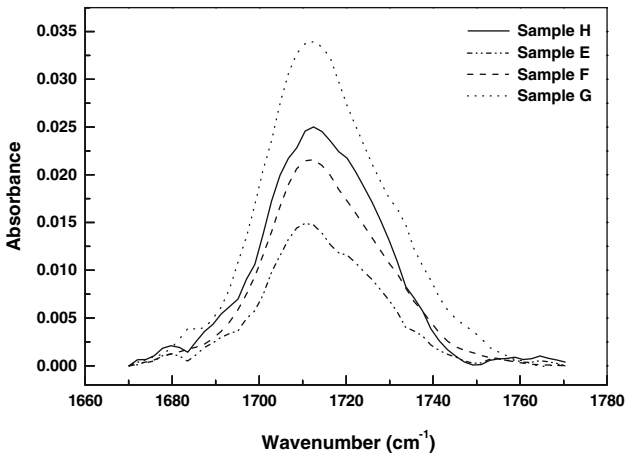

Fig. 10 FTIR-ATR spectra of the Samples E, F, G, and H (films with 70 μm thick), in the region of absorption band at 1,715 cm^{-1}, related to carbonyl groups in α-β-unsaturated compounds

hydroxylation of the aromatic ring. Thus, in a short melting time, primary degradation can occur, forming carboxyl groups and vinyl ester groups, which are bonded to the PET macromolecule, and forming volatile compounds, such as acetaldehyde and formaldehyde, which are not bonded to the PET macromolecule, as already cited. Therefore, it can be assumed that when the processing involves a short melting time, this is not sufficient to promote oxidation reactions in the aromatic ring of the PET and the absorbance intensity of the band at 1,410 cm^{-1} can be used to normalize the absorbance intensity of the band at 1,715 cm^{-1}, as cited in the experimental section. The Sample H was used as a normalizing reference for the comparative analyses with the Samples E, F, and G.

From the absorption intensity band at 1,715 cm^{-1}, normalized with the absorption intensity band at 1,410 cm^{-1}, the relative changes in carboxyl groups on the surfaces of the Samples E, F, and G were estimated, relative to the Sample H.

The results of these analyses are shown in Table 5. No significant differences can be seen in the relative percentage values corresponding to the carboxyl groups for films of Sample G of thickness 70 μm and 270 μm, which indicates that the thickness of the processed PET films did not interfere in the relative increasing of carboxyl groups. Therefore, it is suggested that the relative increasing of carboxyl groups presented in Table 5 could probably be extended to the Samples E, F, and G, which were 2,700 μm thick and used as samples for the depolymerization reaction in non-aqueous alkaline medium [25, 26]. Also, it may be noted that the kind of flow gas used, compressed air or N_2, did not interfere in the relative increasing of carboxyl groups.

Films of Sample G of 70 μm showed a relative increasing in carboxyl groups of 20.0 ± 1.5%, compared

Table 5 Comparative analysis of the changes in the relative increasing in carbonyl band (1,715 cm^{-1}) in the Samples E, F, G, and H

Sample	Amount of water uptake (before thermopressing) (%)[a]	Thickness (μm)	Gas flowing in the FTIR-ATR chamber	Relative increasing in carbonyl band (1,715 cm^{-1}) (%)
H	0.0	70	Compressed air	–
G	0.8 ± 0.1	70	Compressed air	20.0 ± 1.5
E	0.0	70	Compressed air	3.1 ± 0.6
F	0.2 ± 0.1	70	Compressed air	11.3 ± 0.1
H	0.0	270	Compressed air	–
G	0.8 ± 0.1	270	Compressed air	20.3 ± 1.0
H	0.0	70	N_2	–
G	0.8 ± 0.1	70	N_2	20.7 ± 0.3

[a] Compared to film of Sample H

to the films of Sample H. Films of Samples E and F showed 11.3 ± 0.1% and 3.1 ± 0.6%, respectively, compared to film of Sample H. Therefore, from these results, it is observed that the rise in the relative increasing of carboxyl groups on the samples surfaces is directly related to the amount of water taken up by the flakes of recycled PET, before the thermopressing. It is also concluded that this spectroscopic method can be used to determine the relative increasing of carboxyl groups on the surfaces of the Samples E, F, and G.

The absorption intensity band at 1,715 cm^{-1}, which can be related to the structural carbonyl groups in the PET macromolecule (in carboxyl groups at the ends of PET chains and ester groups in the PET backbone), is independent of the length distribution of the PET chains. However, in the present study, it was not possible to evaluate the change in the absorption intensity of the band related to the hydroxyl groups, in the region around 3,200–3,500 cm^{-1}. This was not possible because, according to the theory of FTIR-ATR, the absorption intensity is inversely proportional to the wavenumber. Thus, the absorption intensity band observed for the OH groups was negligible in the region around 3,200–3,500 cm^{-1} and it is not possible to evaluate this absorption region by the FTIR-ATR technique. However, in the studies of thermal and thermooxidative decomposition of Samples E, F, and G, by TG analysis, the formation of polar groups on the surfaces of these samples was detected, especially on the Samples G, which took up more water before thermopressing, due to greater interaction between the O_2 atmosphere in the furnace and the hydrogen atom of the hydroxyl in the carboxyl groups on the surface of this Sample, through hydrogen-bond interactions. Therefore, the FTIR-ATR was useful to evaluate changes in the relative increasing of carboxyl groups on the surfaces of the Samples E, F, and G, relative to Sample H.

From the analyses made and results obtained in this study, it can be confirmed that the reactivity of the Samples G, in an alkaline reaction medium, is related to the amount of carboxyl groups on the surface of them, which accelerate the alkaline depolymerization in the initial reaction stages, as observed in earlier studies carried out by Ruvolo and Curti [25, 26].

Finally, it is needed to highlight that the results obtained in this work, using the compression-molding process, for the PET processing, can be extrapolated to more complex processing, such as extrusion and blow molding. It is possible because the experimental conditions of temperature, presence of oxygen gas and the shear into the equipment during the reaction are experimental parameters more relevant than the processing time. Thus, instead of the extrusion and the blow molding processes need a shorter time to obtain the product than the compression-molding process, in the former the shear is higher than the latter, and in this case the degradation, in presence of the oxygen gas at the melting temperature of the polymer, will be as intense as using the compressing molding. In this way, we consider that both kinds of process can be related.

Conclusions

In DSC analysis, it was shown that the increase in the amount of water taken up by the flakes of recycled PET before processing (Samples A, B, and C) diminished the T_g and T_c of the processed PET samples in the vitreous state (Samples E, F, and G). Also, an exothermic flow of the reminiscent heat was observed in the Samples E, F, and G, between T_c and T_m, which increased with the amount of water taken up by the flakes of recycled PET before processing. The crystallinity index of the Samples E, F, G, and H, determined by DSC, increased as a function of the amount of water taken up, especially after the thermal treatment of the Samples G and H at 180 °C for 4 h (obtaining the Samples I and J). These results suggest that the proportion of short chains is raised as a result of the hydrolytic degradation during thermopressing, which enhances the mobility of the chains of the Samples G

during the thermal treatment and favors the ordering of the polymer segments with short chains.

The study of thermal and thermooxidative decomposition of the Samples G and H showed that the E_a values, determined for thermooxidative decomposition, was higher for the former than for the latter. On the other hand, from the thermal decomposition in an inert atmosphere (N_2), contrary results of E_a were obtained. Once again, this indicates that there is a rise in the proportion of short chains as the amount of water taken up by the flakes of recycled PET before processing increases, and also that the reactivity of these samples increases, due to the formation of carboxyl groups on the polymer surface during thermopressing.

The formation of polar groups on the surfaces of the Samples E, F, and G was confirmed by FTIR-ATR measurements, which indicated a relative rise in the carboxyl groups on the surface of the Sample G, due to the hydrolytic degradation of the flakes of recycled PET (Sample C) during the processing. These results corroborate the DSC and TG analyses.

From the above data and analysis, it can be concluded that increasing amounts of water taken up by the flakes of recycled PET before thermal processing result in higher proportions of short chains in the final plates, due to hydrolytic degradation, which lead to more polar groups being formed on the surfaces of the Samples E, F, and G (carboxyl groups) and can cause a rise in the reactivity of the samples in alkaline reaction medium during the depolymerization reaction, as observed in earlier studies by this group.

References

1. http://www.abepet.com.br/reciclagem, accessed on February 6, 2007
2. http://www.cempre.org.br, accessed on February 6, 2007
3. La Mantia FP, Vinci M (1994) Polym Degrad Stab 45(1):121
4. Torres N, Robin JJ, Boutevin B (2000) Eur Polym J 36(10):2075
5. Spinacé da Silva MA, Paoli de MA (2005) Química Nova 28(1):65
6. Brasil. Agência Nacional de Vigilância Sanitária. Resolução n° 105 – Diário Oficial da República Federativa do Brasil, Seção 1, 21, Brasília-DF, 20 maio (1999). Availabe at: http://www.anvisa.gov.br, accessed on September 15, 2006
7. Yoshioka T, Okayama N, Okuwaki A (1998) Ind Eng Chem Res 37(2):336
8. Yoshioka T, Motoki T, Okuwaki A (2001) Ind Eng Chem Res 40(1):75
9. Mancini SD, Zanin M (2002) Polím: Ciên Tecnol 12(1):34
10. Kao C-Y, Wan B-Z, Cheng W-H (1998) Ind Eng Chem Res 37(4):1228
11. Wan B-Z, Kao C-Y, Cheng W-H (2001) Ind Eng Chem Res 40(2):509
12. Mishra S, Goje AS (2003) Polym React Eng 11(4):963
13. Yang Y, Lu Y, Xiang H, Xu Y, Li Y (2002) Polym Degrad Stab 75(1):185
14. Genta M, Iwaya T, Sasaki M, Goto M, Hirose T (2005) Ind Eng Chem Res 44(11):3894
15. Castro REN, Vidotti GJ, Rubira AF, Muniz EC (2006) J Appl Polym Sci 101(3):2009
16. Hu L-C, Oku A, Yamada E (1997) Polym J 29(9):708
17. Goje AS, Thakur SA, Patil TM, Mishra S (2003) J Appl Polym Sci 90(12):3437
18. Goje AS, Chauhan YP, Mishra S (2004) Polym-Plast Technol Eng 43(1):95
19. Villain F, Coudane J, Vert M (1994) Polym Degrad Stab 43(3):431
20. Ruvolo-Filho A, Carvalho de GM (1999) J Macromol Sci – Phys B 38(3):305
21. Edge M, Wiles R, Allen NS, Mcdonald WA, Mortlock SV (1996) Polym Degrad Stab 53(2):141
22. Dzieciol M, Trzeszczynski J (1998) J Appl Polym Sci 69(12): 2377
23. Campanelli JR, Kamal MR, Cooper DG (1993) J Appl Polym Sci 48(3):443
24. Ruvolo-Filho AC, Soares K (2004) BR Patent, PI 0400074-9, 2004
25. Ruvolo-Filho A, Curti PS (2006) Ind Eng Chem Res 45(24):7985
26. Curti PS, Ruvolo-Filho A (2006) Polím Ciênc Tecnol 26(4):276
27. Oku A, Hu L-C, Yamada E (1997) J Appl Polym Sci 63(5):595
28. Goje AS, Mishra S (2003) Macromol Mat Eng 288(4):326
29. Kumar S, Guria C (2005) J Macromol Sci Part A: Pure Appl Chem 42(3):237
30. Carvalho de GM (2000) Correlação entre comportamento térmico, espessura, propriedades de transporte e a morfologia em filmes de poli(etileno tereftalato). Tese de doutorado, Universidade Federal de São Carlos, SP, Brasil
31. Standard Test Method for Decomposition Kinetics by Thermogravimetry. Método E 1641-99 (ASTM)
32. Sammon C, Yarwood J, Everall N (2000) Polym Degrad Stab 67(1):149
33. Khanna YP, Kuhn WP (1997) J Polym Sci – Part B: Polym Phys 35(14):2219
34. Operation Manual for TGA 2050-TA Instruments
35. Hatakeyama T, Quinn FX (1995) Thermal analysis – fundamentals and applications to polymer science. Wiley, New York
36. Arii T, Ichihara S, Nakagawa H, Fujii N (1998) Thermochim Acta 319(1–2):139
37. Saha B, Ghoshal AK (2005) Chem Eng J 111(1):39
38. Saha B, Maiti AK, Ghoshal AK (2006) Thermochim Acta 444(1):46